Electronic Supplementary Material (ESI) for Catalysis Science & Technology.

Molecular behaviour of phenol in zeolite Beta catalysts as a function of acid site presence: a quasielastic neutron scattering and molecular dynamics simulation study

Carlos Hernandez-Tamargo,[a] Alexander O'Malley,[b,c]* Ian P. Silverwood,[d] and Nora H. de Leeuw[a]*

[a] School of Chemistry, Cardiff University, Main Building, Park Place, Cardiff, CF10 3AT, United Kingdom
[b] The Centre for Sustainable Chemical Technologies (CSCT), Department of Chemistry, University of Bath, Claverton Down, Bath, BA2 7AY, United Kingdom
[c] UK Catalysis Hub, Research Complex at Harwell, Science and Technology Facilities Council Rutherford Appleton Laboratory, Harwell Science and In-novation Campus, Oxon, OX11 0QX, UK
[d] ISIS Pulsed Neutron and Muon Facility, Science and Technology Facilities Council Rutherford Appleton Laboratory, Harwell Science and Innovation Campus, Oxon OX11 0QX, United Kingdom.

Email: a.o'malley@bath.ac.uk, deleeuwn@cardiff.ac.uk

Electronic supplementary information (ESI)

S1. QENS spectra

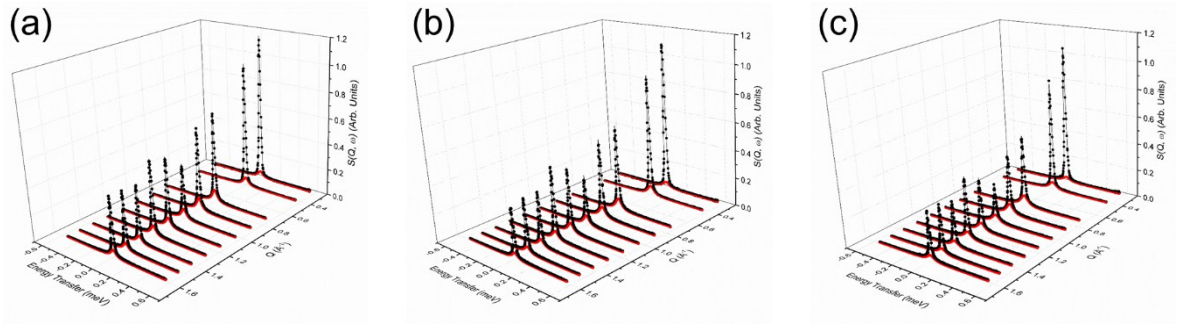

Figure S1. QENS spectra as a function of Q for phenol at (a) 393, (b) 418 and (c) 443 K in zeolite Beta. (–) is the total fit to the data points, (–) is the quasi-elastic Lorentzian component.

S2. Rotational models

In this section we present the analysis of the experimental elastic incoherent structure factor (EISF) to decipher the modes of phenol motion present. Further information on the theory underpinning relevant dynamical models and their application to such systems may be found in the referenced resources.[1,2]

A number of models are available to characterise the localised motions of phenol, related to the geometries of motion of the protons in the molecule. We next outline the models used to fit the experimental EISF.

Isotropic rotation is characterised by a molecule whose reorientation takes place through a series of small angle, random rotations so that no most probable orientation exists on a time average, as depicted in **Figure S2**. The scattering law as derived by Sears (referenced in the main article) for this form of rotation has an EISF ($^{A_0(Q)}$) given as

$$A_0(Q) = j_0^2(Qr) \qquad \textbf{eq. (S1)}$$

where r is the radius of rotation, and j_0 is the 0^{th} order spherical Bessel function given as

$$j_0(Qr) = \frac{\sin(Qr)}{(Qr)} \qquad \textbf{eq. (S2)}$$

The radius of rotation of the 6 protons as calculated from the center of mass is 2.6 Å. The theoretical EISF for isotropic rotation with a radius of rotation of 2.6 Å is plotted against the experimental EISFs in **Figure S3** as the dashed black line. We note that the model falls far below all experimental points.

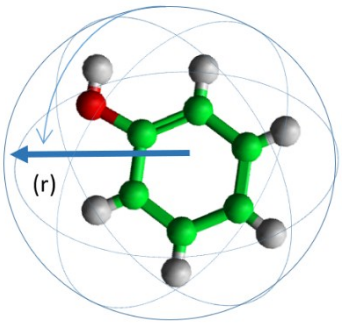

Figure S2. Isotropic rotation of a phenol molecule with a radius of rotation (r).

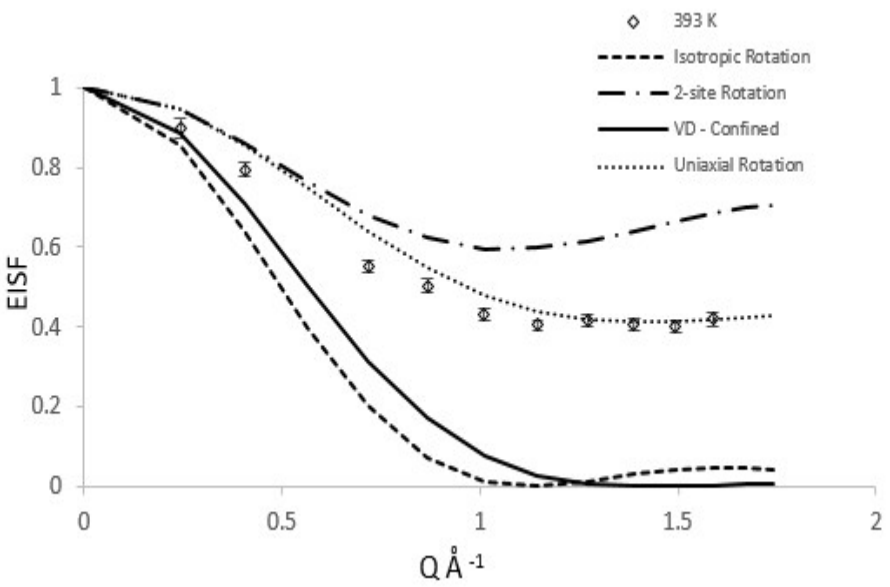

Figure S3. Experimental EISF plot of phenol in zeolite Beta at 393 K against different theoretical EISF models.

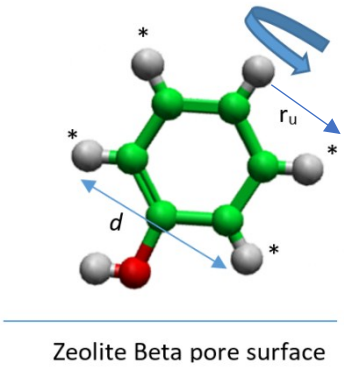

Figure S4. Rotational motion of phenol bound to the zeolite surface by the hydroxyl group. The model depicts 2-site symmetrical rotation of the protons marked with a * around the O-C_1 bond axis with a rotational diameter of *d*, and uniaxial rotation of those same protons around the same axis with a radius of rotation r_u.

Our next consideration is that of a phenol molecule hydrogen-bonded by the O-H group to the zeolite surface, with a rotating benzyl group as shown in **Figure S4**. A model which reasonably describes this motion is that of the rotation of protons which have two-fold rotational symmetry between equivalent sites in a 2-site jump rotation model with a diameter *d*, as depicted in **Figure S4** (marked with an asterisk).

The theoretical EISF of the 2-site jump rotation model is given by **eq. (S3a)**, where j_0 is the 0^{th} order spherical Bessel function in **eq. (S2)**, and *d* in this case is distance between the symmetrically equivalent protons marked by an asterisk in **Figure S4** (4.09 Å).

This model necessitates the incorporation of an immobile fraction (discussed in more detail later when considering entire populations of molecules) as the hydroxyl proton and the proton attached to C_4 are considered static in this model. This incorporation is shown in **eq. (S3b)**, where 4/6 of the protons in the molecule are contributing to the EISF.

$$A_0(Q) = \frac{1}{2}\left[\,1 + j_0(Qd)\right] \qquad \textbf{eq. (S3a)}$$

$$A_0(Q) = \frac{4}{6}\left(\frac{1}{2}\left[\,1 + j_0(Qd)\right]\right) + \left(1 - \frac{4}{6}\right) \qquad \textbf{eq. (S3b)}$$

This model is plotted against the experimental EISF in **Figure S3** as the dot-dashed black line, however it falls above the experimental points for all values of Q. The shape of the model function is also not in agreement with the shape of the experimental EISFs.

We now use the model of continuous uniaxial rotation around a circle to describe the proton motions. This model cannot be used for powder samples typical for porous material studies, because no expression exists for the average angle θ between the axis of rotation and the direction of *Q*. However, with a sufficiently large N (> 7) the scattering function does not change as N increases. The approximation of jump rotation over N sites may then be used, given in **eq. (S4a)**. As with the 2-site jump rotation model, this model necessitates the incorporation of an immobile fraction to account for the hydroxyl proton and the proton attached to C_4 being static in this model, shown in **eq. (S4b)**.

$$A_0(Q) = \frac{1}{N}\sum_{n=1}^{N} j_0\left[\,2Qr_u \sin\left(\frac{n\pi}{N}\right)\right] \qquad \textbf{eq. (S4a)}$$

$$A_0(Q) = \frac{4}{6}\left(\frac{1}{N}\sum_{n=1}^{N} j_0\left[\,2Qr_u \sin\left(\frac{n\pi}{N}\right)\right]\right) + \left(1 - \frac{4}{6}\right) \qquad \textbf{eq. (S4b)}$$

This model is plotted against the experimental EISF as the dotted line in **Figure S3**; while this plot appears to fit the data at the highest Q values, it falls above the experimental points outside of the error bars at Q values below 1.27 $Å^{-1}$.

We now consider translational motion of the oxime localised to a confined volume. Volino and Dianoux (referenced in the main article) developed a model to describe a scattering molecule undergoing translational motions in a confined spherical volume of radius r_{conf} (shown in **Figure S5**). This scattering model is based on the general problem of a particle diffusing in a potential field of spherical symmetry, where the potential is low inside the sphere's volume but infinite outside of it.

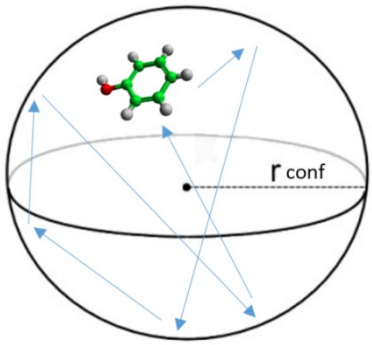

Figure S5. Translational motion of the cyclohexanone oxime confined to a sphere of radius r_{conf}.

The EISF of this model is given as:

$$A_0(Q) = \left[\frac{3j_1(Qr_{conf})}{Qr_{conf}}\right]^2 \qquad \textbf{eq. (S5)}$$

where j_1 is the spherical Bessel function of the first kind, order 1, given by:

$$j_1(Qr_{conf}) = \frac{\sin(Qr_{conf})}{(Qr_{conf})} - \frac{\cos(Qr_{conf})}{(Qr_{conf})} \qquad \textbf{eq. (S6)}$$

where r_{conf} is the radius of the sphere which confines the diffusion. In this study we consider the radius of a micro-pore in zeolite Beta, 3.3 Å. The Volino model for confined diffusion is plotted in **Figure S3** as the solid black line, showing that the model falls below the experimental points at all Q values.

The localised models alone are clearly not suitable for fitting the EISF. However, we may also consider that only a fraction of molecules is mobile and undergoing such localised motions on the timescale of the instrument, with the remaining molecules considered as static, potentially bound through strong hydrogen-bonding to the zeolite Brønsted acid sites. We can calculate an effective EISF which takes this scenario into consideration, given by:

$$A_{0\_eff}(Q) = p_x A_0(Q) + (1 - p_x) \qquad \textbf{eq. (S7)}$$

where p_x is the fraction of mobile molecules, and $A_0(Q)$ is each EISF as shown in **eq. (S1)**, **eq. (S3b)**, **eq. (S4b)**, and **eq. (S5)**. In **Figure S6** we plot these effective EISFs against the experimental data obtained at 393 K with the optimal p_x (as obtained by a least squares fitting procedure). While the 2-site jump rotation model is not able to provide an adequate fit at any fraction, we observe that both the isotropic rotation model and the Volino confined diffusion model give agreement within the error bars of the experimental data points, when a mobile fraction of 0.6 and 0.55 are implemented respectively.

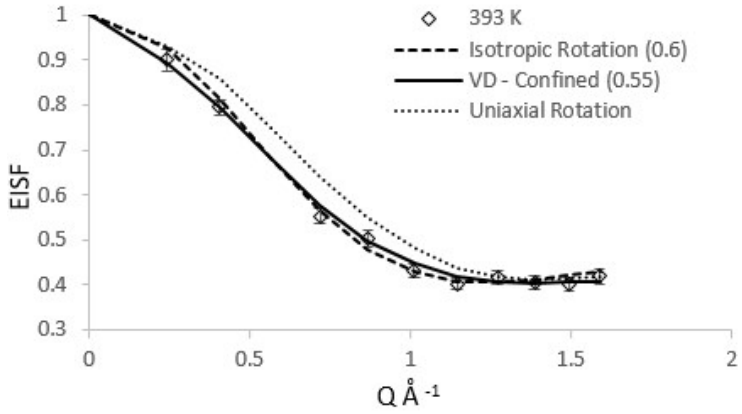

Figure S6. The experimental EISF of phenol in zeolite Beta at 393 K, plotted against the models of localised motions after fitting with an immobile fraction. The optimum p_x value is listed in brackets.

The close agreement to the experimental data of both the isotropic rotation model and the confined diffusion model leaves ambiguity as to which form of motion is observed. However, this ambiguity may be addressed by examining the broadenings of the QENS spectra as a function of *Q*. The full width at half maximum (FWHM) of the Lorentzian component of the QENS spectra as a function of *Q* at 393 K are plotted in **Figure S7**. Crucially, the plot shows

that the broadenings are independent of *Q*, which discounts the possibility of any dynamical behaviour involving translational motion being observed on the timescale of the instrument, including diffusion confined to a spherical volume. Had Fickian diffusion confined to a spherical volume been present, the broadenings would have shown a DQ^2 dependence, with a plateauing at *Q* values below $Q = \pi/r_{conf}$ (which in this case would be 0.95 $Å^{-1}$ if we consider r_{conf} to be 3.3 Å). Had the motion been of the nature of jump diffusion confined to a spherical volume, the broadenings would have exhibited a dependence such as that in previous work,[88] where a *Q* dependence of one of the relevant jump diffusion models would be exhibited, but with the same plateauing below *Q* = 0.95. The absence of such a dependence allows us to conclude that we are observing isotropic rotation of phenol in the zeolite Beta channels with a fraction of immobile molecules.

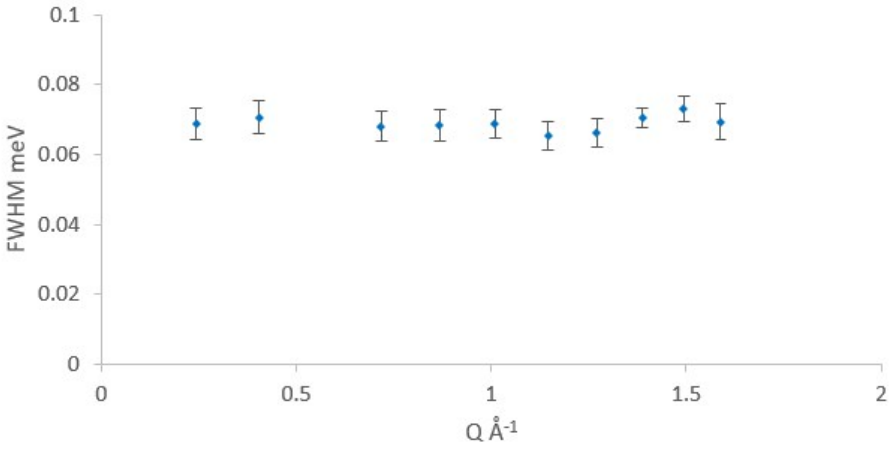

Figure S7. Q-dependence of the HWHM broadening of the Lorentzian components of QENS spectra of phenol in zeolite Beta at 393 K.

References:

1. M. Bee, Quasielastic neutron scattering: principles and applications in solid state chemistry, *Biology and Materials Science*, Adam Hilger, Bristol, 1988
2. A. J. O'Malley and C. R. A. Catlow, in *Experimental Methods in the Physical Sciences*, Academic Press, 2017, vol. 49, pp. 349–401